Allylic Alcohol Epoxidation by Methyltrioxorhenium: A Density Functional Study on the Mechanism and the Role of Hydrogen Bonding

Cristiana Di Valentin,[†] Remo Gandolfi,*[,†] Philip Gisdakis,[‡] and Notker Rösch*[,‡]

Contribution from the Department of Organic Chemistry, University of Pavia, 27100 Pavia, Italy, and Institut für Physikalische und Theoretische Chemie, Technische Universität München, 85747 Garching, Germany

Received November 3, 2000. Revised Manuscript Received January 4, 2001

Abstract: By locating all relevant transition structures with a hybrid density functional method, we explored the three most reasonable mechanisms for H_2O_2 epoxidation of propenol catalyzed by methyltrioxorhenium (MTO), namely: (i) coordination of propenol as lone pair donor to rhenium mono- and bis-peroxo complexes followed by intramolecular epoxidation, (ii) formation of a metal alcoholate, derived from addition of propenol to the Re complex with the formation of a metal−OR bond, followed by intramolecular epoxidation, (iii) intermolecular oxygen transfer assisted by hydrogen bonding where the rhenium complex acts as hydrogen bond acceptor and HOR as hydrogen bond donor. The computational results demonstrate that the last route is highly favored over the other two and, in particular, they provide the first unambiguous and compelling evidence that alcoholate−metal complexes, mechanism (ii), do not appreciably contribute to product formation. In keeping with experimental findings, theoretical data predict that the monoperoxo Re complex should be considerably less reactive than its bis(peroxo) counterpart and suggest that the hydrated form of the latter complex should be the actual active epoxidant species. All transition structures exhibit a distorted spiro-like structure, while the most stable ones feature hydrogen bonding to the attacking peroxo fragment with the olefinic OH group either in an "outside" ($OC_1C_2C_3 \approx 128°$) or "inside" ($OC_1C_2C_3 \approx 14°$) conformation. Previous qualitative models for transition structures of Re-catalyzed epoxidation of allylic alcohols are discussed in the light of our computational data.

Introduction

Olefin epoxidation catalyzed by transition metal peroxo complexes is a well-established synthetic strategy.[1] Allylic alcohols form a very interesting class of substrates for epoxidation because they produce epoxides with a hydroxyl group as an additional functional group that is able to play an important role in the subsequent building of complex molecules.[2] This synthetic aspect certainly benefits from the hydroxy-group-directed selectivity of oxygen delivery.

It has become increasingly evident that methyltrioxorhenium (MTO) **1** is a particularly appealing catalyst for oxygen transfer from H_2O_2 to olefin (Schemes 1−3) owing to the simplicity, efficiency, versatility, and selectivity of this reaction.[3,4] The growing synthetic use of this protocol obviously stimulated extensive experimental mechanistic investigations [3−6] which, in turn, triggered recent computational studies.[4,7,8] Several points were addressed in this debate:

Scheme 1

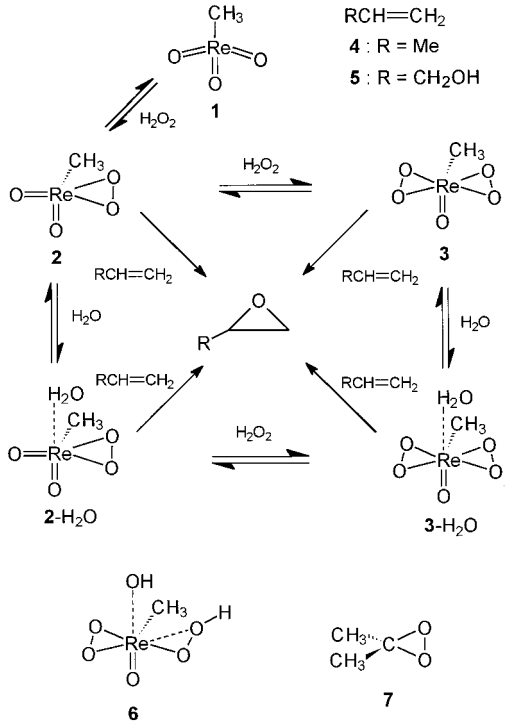

[†] University of Pavia.

[‡] Technische Universität München.

(1) Jira, R.; Sheldon, R. A. In *Applied Homogeneous Catalysis with Organometallic Compounds*; Cornils, B., Herrmann, W. A., Eds.; Wiley-VCH: Weinheim, 1996; Vol. 1, p 374.

(2) Hanson, R. M. *Chem. Rev.* **1991**, *92*, 437.

(3) (a) Romão, C. C.; Kühn, F. E.; Herrmann, W. A. *Chem. Rev.* **1997**, *97*, 3197. (b) Espenson, J. H.; Abu-Omon, M. M. *Adv. Chem. Ser.* **1997**, *253*, 99. (c) Gable, K. P. *Adv. Organomet. Chem.* **1997**, *41*, 127. (d) Herrmann, W. A.; Kühn, F. E. *Acc. Chem. Res.* **1997**, *30*, 169−180. For more recent literature: (e) Wang, W.; Espenson, J. H. *J. Am. Chem. Soc.* **1998**, *120*, 11335. (f) Herrmann, W. A.; Kratzer, R. M.; Ding, H.; Thiel, W. R.; Glas, H. *J. Organomet. Chem.* **1998**, *555*, 293. (g) Tan, H. Espenson, J. H. *Inorg. Chem.* **1998**, *37*, 467. (h) Adam, W.; Stegmann, R. V.; Saha-Möller, C. R. *J. Am. Chem. Soc.* **1999**, *121*, 1879.

(4) Kühn, F. E.; Santos, A. M.; Roesky, P. W.; Herdtweck, E.; Scherer, W.; Gisdakis, P.; Yudanov, I. V.; Di Valentin, C.; Rösch, N. *Chem. Eur. J.* **1999**, *5*, 3603.

10.1021/ja003868y CCC: $20.00
Published on Web 02/15/2001

Scheme 2

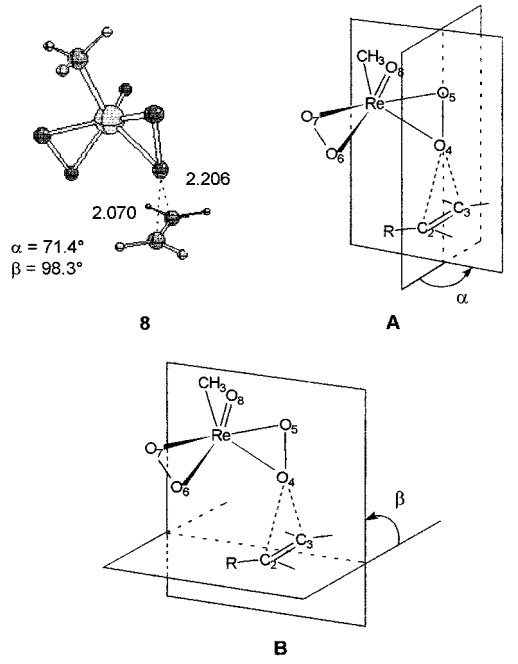

Scheme 3

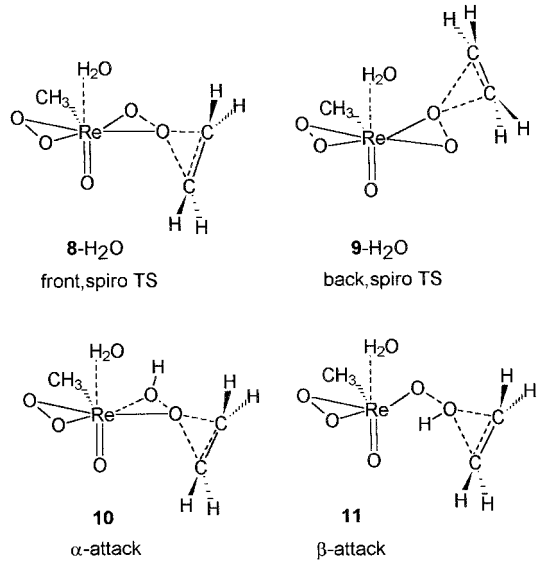

(i) the relative reactivity and consequently the role played in epoxidation by the monoperoxo form **2** and the bis(peroxo) complex **3** (Scheme 1),

(ii) the ability of a base ligand, occupying the seventh coordination site (see **2**-H_2O and **3**-H_2O in Scheme 1), to stabilize the complexes and alter their reactivity,

(iii) the preference for the attack at the front-side oxygen of the reacting peroxo bridge versus that at the backside oxygen, for example, front-spiro (**8**-H_2O) and back-spiro (**9**-H_2O) transitition structures (TSs) respectively, involving the distal (away from the methyl ligand) and proximal oxygen, Scheme 3, and

(iv) the possible role, if any, of hydroperoxo complexes (**6**, Scheme 1) involving the α (**10**) or *β* (**11**) oxygen centers (Scheme 3) of the hydroperoxo moiety.

By now it has not been definitely assessed to what extent the bis(peroxo) complex is catalytically more active as oxidant than the monoperoxo derivative. As far as alkene epoxidation is concerned, the bis(peroxo) form (**3**-H_2O, which has been characterized by X-ray and shown to be catalytically active) has been described by experimentalists either as far more reactive[5b] or as somewhat faster than the monoperoxo form.[6a] The two species have also been considered to be "comparably active".[6b]

As for theoretical analysis, Rösch et al.[7,9] (taking into account hydration and peroxidation energies as well as epoxidation activation energies) concluded that hydrated monoperoxo **2**-H_2O and bis(peroxo) **3**-H_2O complexes are likely to compete with each other (with the latter possibly more reactive) and that selection among the reaction routes may also be influenced by entropic effects and reaction conditions.

Calculations indicate that epoxidation TSs of all peroxo forms exhibit a spiro-like structure,[7] that is, with the peroxo−Re plane almost perpendicular to the C═C bond. In other words the value of the dihedral angle (α, Scheme 2) between the peroxo−Re plane and the forming oxirane plane is not too far from 90°, for example, 71° in TS **8** for **3** + ethene (Scheme 2). The electrophilic concerted attack of the Re complex on the alkene[4,10] gives rise to a significant transfer of electronic charge from the alkene to the Re complex, driven by the dominant frontier orbital interaction, that is, π(C═C)−σ*(O−O).[9,11] The two oxygens of the peroxo moiety exhibit different reactivity: the proximal peroxo oxygen center (that adjacent to the methyl group) is more reactive than the distal one in the monoperoxo form, while the opposite holds for the bis(peroxo) derivative.

A water ligand coordinated at the rhenium center (e.g., **3**-H_2O, water is always present in the reaction mixture) was calculated to strongly stabilize not only the peroxo complex, for example**,** **3** (the energy of **3**-H_2O is lower than that of **3** by 16.3 kcal/mol)[7] but also the corresponding epoxidation TSs (e.g., TS **8**-H_2O is more stable than TS **8** by 12.5 kcal/mol). The former effect prevails with a resultant increase in activation energy of the epoxidation step on passing from the reaction of bis(peroxo) complex **3** to that of its hydrated form **3**-H_2O (namely, from 12.4 to 16.2 kcal/mol in ethene epoxidation).[7] However, the hydrated TS **8**-H_2O exhibits a lower (by 12.5 kcal/mol) absolute energy than the corresponding unsolvated TS **8,** and it was concluded that epoxidation by the bis(peroxo) derivative actually proceeds via the former TS. An added base, such as pyridine or pyrazole, can extrude the water ligand from complex **3**-H_2O, however; at the same time, it stabilizes even more the related epoxidation TS (e.g., on passing from **8**-H_2O to **8**-pyridine) with a consequent beneficial effect on the epoxidation rate in agreement with experimental data.[4]

While there is general consensus in assigning the hydrated complex **3**-H_2O as the epoxidant form in the epoxidation through the bis(peroxo)−Re complex,[4,6,12] either the hydrated (**2**-H_2O)[5,12] or the water-free derivative (**2**)[6,13] has been chosen for the reaction via the monoperoxo complex.

(5) (a) Herrmann, W. A.; Fisher, R. W.; Scherer, W.; Rauch, M. U. *Angew. Chem., Int. Ed. Engl.* **1993**, *32*, 1157. (b) Herrmann, W. A. *J. Organomet. Chem.* **1995**, *500*, 149.

(6) (a) Al-Ajlouni, A.; Espenson, J. H. *J. Am. Chem. Soc.* **1995**, *117*, 9243. (b) Al-Ajlouni, A.; Espenson, J. H. *J. Org. Chem.* **1996**, *61*, 3969.

(7) Gisdakis, P.; Antonczak, S.; Köstlmeier, S.; Herrmann, W. A.; Rösch, N. *Angew. Chem., Int. Ed. Engl.* **1998**, *110*, 2211.

(8) Wu, Y.; Sun, J. *J. Org. Chem.* **1998**, *63*, 1752.

(9) Gisdakis, P.; Rösch, N. Manuscript submitted.

(10) The barrier for rotation of the ethene C═C bond relative to the Re−O−O plane (angle α in Scheme 4 **A**) in the epoxidation transition state is smaller, about 4.6 kcal/mol, (Di Valentin, C.; Gisdakis, P.; Rösch, N., unpublished results) than that in the corresponding transition state of dioxirane where the barrier is calculated to be about 7.4 kcal/mol.[20a]

(11) Rösch, N.; Gisdakis, P.; Yudanov, I. V.; Di Valentin, C. In *Peroxide Chemistry: Mechanistic and Preparative Aspects of Oxygen Transfer*; Adam, W., Eds.; Wiley-VCH: Weinheim, 2000, 601−619.

Scheme 4

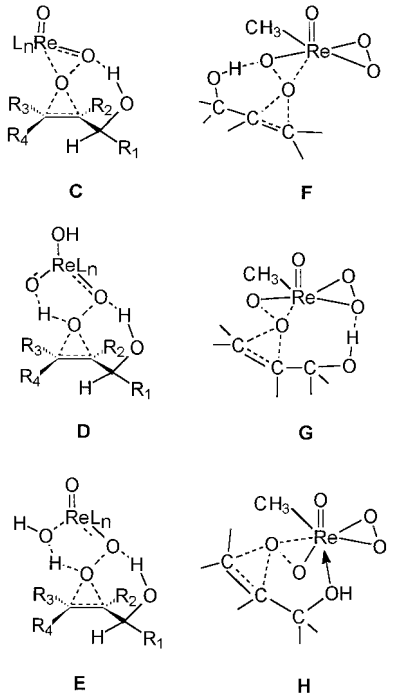

Activation barriers for transition structures of spiro attacks on hydroperoxo derivative of Re (e.g., **6**, Scheme 1) by ethene are rather large and somewhat higher than those involving the peroxo forms.[7,9] Thus, this finding makes it improbable that attacks to either α or β (the less reactive) oxygen centers of a hydroperoxo complex (e.g., **10** and **11**) play competitive roles in Re-catalyzed epoxidation of simple alkenes.

In the case of epoxidation of allylic alcohols, several new mechanistic degrees of freedom have to be considered, in particular, competition among three conceivable reaction routes: (i) coordination of the allylic alcohol (as lone pair donor) to the rhenium complex followed by intramolecular epoxidation, (ii) formation of a metal−alcoholate (derived from addition of the allylic alcohol to the complex with formation of a metal−OR bond) followed by a stereocontrolled intramolecular oxygen delivery by the peroxo group, and (iii) an intermolecular oxygen transfer process assisted, already at the start of the reaction and even more so in the transition state, by a hydrogen-bonding interaction in which the rhenium complex acts as hydrogen bond acceptor and HOR as hydrogen bond donor. Hydrogen bonding could deeply alter the TS geometry observed in the epoxidation of simple alkenes.

Adam and co-workers[12,14] have produced very interesting regioselectivity and face selectivity data for the epoxidation of acyclic and cyclic allylic alcohols aimed at elucidating the reaction mechanism and assessing approximate TS geometries. They stressed that regio- and diastereoselectivity as well as the protic solvent effects observed in these reactions can be satisfactorily explained only on the basis of hydrogen-bonding interaction while these results seem to be definitely at variance with the formation of an alcoholate derivative. They considered three types of TSs (Scheme 4), namely the dioxirane- (**C**), peracid- (**D**), and perhydrate-type (**E**) TSs; the first one involves a peroxo−Re complex, while the other two exhibit a hydroperoxo−Re complex. The face selectivity observed with chiral allylic alcohols seems to better comply with **D**-type (or **E**-type) TSs and with $OC_1C_2C_3$ dihedral angles of ∼120 °C, which, in opinion of these authors,[15,16] are typical for TSs of peroxyacid epoxidations of allylic alcohols. However, Adam and co-workers adhered to the generally accepted rhenium−(mono or bis)peroxo complexes as the active epoxidant species via TS **C**. In all three types of TSs, hydrogen bonding involves that oxygen center of the reacting peroxo moiety which is not directly involved in the oxygen transfer (i.e., O_5 of our numbering scheme).

Although not explicitly underlined, the TSs **C**−**E** as depicted previously[15,16] feature a planar geometry, that is, the forming oxirane plane coincides with the peroxo−Re (**C**) or peroxy−Re plane (**D**, **E**) (Scheme 4). Thus, the question arises whether the tendency to maximize hydrogen bonding can force the reacting system to choose the inherently less stable planar transition structure, given that (as mentioned above) simple alkenes prefer TSs with spiro geometry.

Recall that high-level calculations have demonstrated that TSs for peroxyacid epoxidation of cyclic and acyclic alcohols adopt a spiro geometry similar to that calculated for epoxidation of simple alkenes.[17−19] Spiro TSs are also typical for dioxirane (e.g., dimethyldioxirane **7,** Scheme 1) epoxidations of both alkenes and allylic alcohols[20,21] and for alkene epoxidation by various metal−peroxo complexes (Ti,[22] Mo, W,[23] and Re[7]).[10]

Very recently, Espenson and co-workers[24] reported a noteworthy kinetic study on MTO epoxidation of allylic alcohols. In addition to demonstrating that allylic alcohols react more slowly than their hydrocarbon analogues (2-cyclohexen-1-ol reacted 6 times more slowly than 3-methyl-1-cyclohexene), this study provided, as stated by the authors, a striking result: only the rhenium−bis(peroxo) complex was the active epoxidant species, while the monoperoxo derivative appeared to be of negligible importance. They discussed three TSs (**F**, **G**, and **H**, Scheme 4) and concluded that only TS **G** can satisfactorily explain the much higher reactivity of the bis(peroxo) than the monoperoxo form. In fact, either hydrogen bonding or coordination of the OH group to the rhenium atom (present in **F** and **H**, respectively) can be operative both for monoperoxo and bis(peroxo) species, while hydrogen bonding between the OH group and the O atom of another peroxo group (as in **G)** is possible only for the bis(peroxo)−rhenium complex.

Is quite evident that the proposed qualitative TS models **C** and **G** (Scheme 4) not only leave open many mechanistic questions and look somewhat too schematic, but also do not

(12) (a) Adam, W.; Mitchell, C. M.; Saha-Möller, C. R. *J. Org. Chem.* **1999**, *64*, 3699. (b) Adam, W.; Mitchell, C. M.; Saha-Möller, C. R. *Eur. J. Org. Chem.* **1999**, *785*, 5.

(13) Yudin, A. K.; Sharpless, K. B. *J. Am. Chem. Soc*. **1997**, *119*, 11536.

(14) Adam, W.; Mitchell, C. M. *Angew. Chem., Int. Ed. Engl.* **1996**, *35*, 533.

(15) (a) Adam, W.; Mitchell, C. M.; Saha-Möller, C. R. *J. Org. Chem.* **1999**, *64*, 3699. (b) Adam, W., Mitchell, C. M.; Saha-Möller, C. R. *Eur. J. Org. Chem.* **1999**, *785*, 5.

(16) Adam, W.; Mitchell, C. M. *Angew. Chem., Int. Ed. Engl.* **1996**, *35*, 533.

(17) (a) Singleton, D. A.; Merrigan, S. R.; Liu, J.; Houk, K. N. *J. Am. Chem. Soc.* **1997**, *119*, 3385. (b) Bach, R. D.; Glukhovtsev, M. N.; Gonzales, C. *J. Am. Chem. Soc.* **1998**, *120*, 9902.

(18) (a) Freccero, M.; Gandolfi, R.; Sarzi-Amadè, M.; Rastelli, A. *J. Org. Chem.* **1999**, *64*, 3853. (b) Bach, R. D.; Estévez, C. M.; Winter, J. E.; Glukhovtsev, M. N. *J. Am. Chem. Soc*. **1998**, *120*, 680.

(19) Freccero, M.; Gandolfi, R.; Sarzi-Amadè, M.; Rastelli, A. *J. Org. Chem.* **2000**, *65*, 2030 and 8948.

(20) (a) Houk, K. N.; Liu, J.; DeMello, N.; Condroski, K. R. *J. Am. Chem. Soc.* **1997**, *117*, 8586, 10147. (b) Freccero, M.; Gandolfi, R.; Sarzi-Amadè, M.; Rastelli, A. *Tetrahedron* **1998**, *54*, 6123.

(21) Freccero, M.; Gandolfi, R.; Sarzi-Amadè, M.; Rastelli, A. *Tetrahedron* **1998**, *54*, 12323.

(22) Yudanov, I. V.; Gisdakis P.; Di Valentin C.; Rösch N. *Eur. J. Inorg. Chem.* **1999**, *1999*, 2135.

(23) Di Valentin, C.; Gisdakis, P.; Yudanov, I. V.; Rösch, N. *J. Org. Chem.* **2000**, *65*, 2996.

(24) Tetzlaff, H. R.; Espenson, J. H. *Inorg. Chem.* **1999**, *38*, 881.

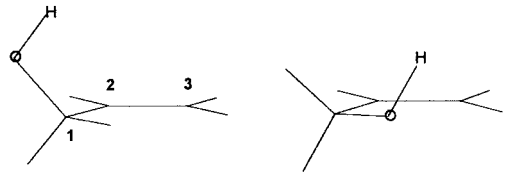

out-**5a** (0.00) in-**5b** (0.49)

$OC_1C_2C_3$ 126.8° 8.7°
HOC_1C_2 -55.9° 57.3°

Figure 1. The two most stable conformers of 2-propen-1-ol with their relative energies (kcal/mol) at the B3LYP/6-311+G* level.

agree with each other. The steadily increasing synthetic relevance of MTO-catalyzed epoxidations and the related mechanistic interest make it necessary to have reliable transition structures that provide landmarks useful to orient experimentalists in discussing (rationalizing and predicting, if possible) reaction rates as well as selectivity of these reactions.

In the present computational study employing DFT-based methods we aimed to precisely define geometries and relative energies (gas phase) of transition structures (TSs) for the MTO-catalyzed epoxidation of the parent allylic alcohol, that is, propenol, in which steric effects are missing as far as possible. In particular we were interested

(i) in assessing which interaction (hydrogen bonding, metal−alcoholate formation, or metal−alcohol coordination) between the allylic OH and the rhenium complex is operative in TSs,

(ii) in determining which oxygen of the Re−peroxo complex acts, in the case of hydrogen-bonded TSs, as hydrogen-bond acceptor,

(iii) in exactly defining the value of the torsion angle $OC_1C_2C_3$ (Figure 1) claimed to be decisive for reaction stereocontrol[25] and considered to be ∼120−130° in TS models for Re-catalyzed epoxidation,[12,26] and

(iv) in answering the question why allylic alcohols are less reactive than related alkenes or, in other words, why the energy stabilization due to hydrogen bonding does not override the rate-retarding electron-withdrawing effect of the hydroxy group.

Computational Methods

We carried out density functional calculations employing the hybrid B3LYP scheme[27] to describe the exchange-correlation contribution to the electron−electron interaction. This method is now well established as a method that can reliably describe potential energy surfaces for epoxidation reaction with transition metal−peroxo complexes.[28] Geometries of intermediates and TSs were initially optimized with a small basis set (LanL2DZ) and transition-state structures were checked by performing a full vibrational analysis at this level of theory. The basis set was then enlarged. LanL2 effective core potentials[29] were used to replace the core electrons of Re (except for the outermost shells). The corresponding basis sets for the valence and the outermost core electrons of the transition elements were used in the contraction (441/2111/21). For main group elements we employed the rather flexible basis set 6-311G(d,p).[30] This computational strategy has been discussed in detail elsewhere[31a] and, following that nomenclature of basis sets, it will be referred to as basis set IIb. All geometry optimizations of intermediates and transition structures were performed without any symmetry constraints. The transition-state structures were searched by numerically estimating the matrix of the second-order energy derivatives at every optimization step and by requiring only one eigenvalue of this matrix to be negative.

Energies of stationary points were then refined in single-point fashion[31] first by augmenting the Re basis set by two f-type polarization exponents (0.5895 and 0.2683) (IIIb//IIb) and then by further adding diffuse functions, that is, by using the basis set 6-311+G(d,p) for main group elements (III′b//IIb). Throughout this work, the latter basis sets are referred to as IIIb and III′b, respectively.[31] With these flexible basis sets, the B3LYP method affords an acceptable description of lone pairs and hydrogen-bonding interactions.[32]

The natural bond orbital approach (NBO) was used to analyze atomic charges.[33] All calculations were performed with the Gaussian 94[34] and Gaussian 98 suites of programs.[35]

Relevant structural data of the TSs of propene and propenol epoxidation with **3** are collected in Table 2 (and in Table S2 of the Supporting Information). Data for other intermediates and TSs are available on request.

Electronic energies of reactants, intermediates and transition structures (TSs) (from both IIIb and III′b calculations) are reported in Tables 1 and 3−5 (see also Tables S1 and S3−S5, Supporting Information). In the discussion we will rely on the energies of higher-level calculations. Vibrational zero-point energies (ZPE) of isomeric TSs from LanL2DZ calculations were found similar to each other; they are provided in Tables S1 and S3−S5 (Supporting Information).

For the sake of clarity and to allow uniform comparison, we quote all energies (designated as E_{rel} in Tables 1 and 3−5) of intermediates and transition structures, for all three mechanisms, relative to the same

(25) (a) Adam, W.; Smerz, A. K. *J. Org. Chem.* **1996**, *61*, 3506. (b) Adam, W.; Kumar, R.; Reddy, T. I.; Renz, M. *Angew. Chem., Int. Ed. Engl.* **1996**, *35*, 880.

(26) Adam, W.; Wirth, T. *Acc. Chem. Res.* **1999**, *32*, 703.

(27) (a) Becke, A. D. *J. Chem. Phys.* **1993**, *98*, 1372. (b) Lee, C.; Yang, W.; Parr, R. G. *Phys. Rev. B* **1988**, *37*, 785.

(28) Görling, A.; Trickey, S. B.; Gisdakis, P.; Rösch, N. In *Topics in Organometallic Chemistry*; Brown, J., Hofmann, P., Eds.; Springer: Heidelberg, 1999; Vol. 4, p 109.

(29) (a) Hay, P. J.; Wadt, W. R. *J. Chem. Phys.* **1985**, *82*, 299. (b) Frenking, G.; Antes, I.; Böhme, M.; Dapprich, S.; Ehlers, A. W.; Jonas, V.; Neuhaus, A.; Otto, M.; Stegmann, R.; Veldkamp, A.; Vyboishchikov, S. F. In *Reviews in Computational Chemistry*; Lipkowitz, K. B., Boyd, D. B., Eds.; VCH: New York, 1996; Vol. 8, p 63.

(30) (a) Krishnan, R.; Binkley, J.; Seeger, R.; Pople, J. *J. Chem. Phys.* **1980**, *72*, 650. (b) McLean, A.; Chandler, G. *J. Chem. Phys.* **1980**, *72*, 5639.

(31) (a) Gisdakis, P.; Antonczak, S.; Rösch, N. *Organometallics* **1999**, *18*, 5044. (b) Full geometry optimization of TS **21** and **25** with the IIIb and III′b basis sets demonstrated the following. (i) Only small differences in Re−O bond lengths (<0.02 Å) are observed on passing from basis set IIb to basis set IIIb while introduction of diffuse functions (basis set III′b) brings about a further slight (<0.02 Å) change in incipient bond lengths (i.e., TS geometries do not strongly depends on the basis set used). (ii) Absolute energies obtained by full optimization with basis sets IIIb and III′b are lower by 1−2 kcal/mol than those obtained by single-point calculations IIIb//IIb and III′b//IIb, respectively, while relative energies are very similar, e.g., E(**25**) − E(**21**) = 0.59 (0.02) and 0.73 (0.20) kcal/mol for IIIb (III′b) and IIIb//IIb (III′b//IIb) calculations, respectively. These observations strongly suggest that energies refined in single-point fashion can be considered acceptable.

(32) (a) Pan, Y.; Mc. Allister, M. A. *J. Am. Chem. Soc.* **1998**, *120*, 166. (b) Pudzianowski, A. T. *J. Phys. Chem.* **1996**, *100*, 4781. (c) Del Bene, J. E.; Person, W. B.; Szczepaniak, K. *J. Phys. Chem.* **1995**, *99*, 10705.

(33) Reed, A. E.; Curtiss, L. A.; Weinhold, F. *Chem. Rev.* **1988**, *88*, 899.

(34) Frisch, M. J.; Trucks, G. W.; Schlegel, H. B.; Gill, P. M. W.; Johnson, B. G.; Robb, M. A.; Cheeseman, J. R., Keith, T.; Petersson, G. A.; Montgomery, J. A.; Raghavachari, K.; Al-Laham, M. A.; Zakrzewski, V. G.; Ortiz, J. V.; Foresman, J. B.; Cioslowski, J.; Stefanov, B. B.; Nanayakkara, A.; Challacombe, M.; Peng, C. Y.; Ayala, P. Y.; Chen, W.; Wong, M. W.; Andres, J. L.; Replogle, E. S.; Gomperts, R.; Martin, R. L.; Fox, D. J.; Binkley, J. S.; Defrees, D. J.; Baker, J.; Stewart, J. P.; Head-Gordon, M.; Gonzalez, C.; Pople, J. A. *Gaussian 94*, revision D.3; Gaussian, Inc.: Pittsburgh, PA, 1995.

(35) Frisch, J.; Trucks, G. W.; Schlegel, H. B.; Scuseria, G. E.; Robb, M. A.; Cheeseman, J. R.; Zakrzewski, V. G.; Montgomery, J. A., Jr.; Stratmann, R. E.; Burant, J. C.; Dapprich, S.; Millam, J. M.; Daniels, D.; Kudin, K. N.; Strain, M. C.; Farkas, O.; Tomasi, J.; Barone, V.; Cossi, M.; Cammi, R.; Mennucci, B.; Pomelli, C.; Adamo, C.; Clifford, S.; Ochterski, J.; Petersson, G. A.; Ayala, P. Y.; Cui, Q.; Morokuma, K.; Malick, D. K.; Rabuck, A. D.; Raghavachari, K.; Foresman, J. B.; Cioslowski, J.; Ortiz, J. V.; Stefanov, B. B.; Liu, G.; Liashenko, A.; Piskorz, P.; Komaromi, I.; Gomperts, R.; Martin, R. L.; Fox, D. J.; Keith, T.; Al-Laham, M. A.; Peng, C. Y.; Nanayakkara, A.; Gonzalez, C.; Challacombe, M.; Gill, P. M. W.; Johnson, B.; Chen, W.; Wong, M. W.; Andres, J. L.; Head-Gordon, M.; Replogle, E. S.; Pople, J. A. *Gaussian 98*, revision A.6; Gaussian, Inc.: Pittsburgh, PA, 1998.

Table 1. Relative Energies (E_{rel}) and Activation Barriers ($\Delta E^{\ddagger}$) for Intermediates (**I-12**−I-**17**-H_2O) and Transition Structures (**S-12**−**S-17**-H_2O) Characterized by Either Alcohol Coordination or Alcoholate−Metal Binding[a]

	E_{rel}[b] kcal/mol		E_{rel}[b] kcal/mol	$\Delta E^{\ddagger}$[c,d] kcal/mol
3 + **5a** + H_2O	0.0			
3-H_2O + **5a**	−12.0			
I-12	−11.4	**S-12**	15.2	26.6
I-13-H_2O	−13.3	**S-13**−H_2O	6.0	19.3
I-14	15.8	**S-14**	36.3	20.5
I-15	9.2	**S-15**	29.6	20.4
I-16-H_2O	22.0	**S-16**−H_2O	45.4	23.4
I-17H_2O	−6.2	**S-17**−H_2O	28.5	34.7

[a] B3LYP/III′b//B3LYP/IIb calculations. [b] E_{rel} are referred to the sum of the reactant energies, i.e., E(**3**) (−495.166170 hartree) + E(**5a**) (−193.182995 hartree) + E(H_2O) (−76.458463 hartree) = −764.807628 hartree. E_{rel} of water-free **I** and **S** includes the energy of a free water molecule. [c] $\Delta E^{\ddagger}$ are relative to the corresponding starting intermediate. [d] ZPE values of isomeric TSs are very similar to each other (for **S-12**, **S-14**, **S-15** about 87 kcal/mol and for **S-13**-H_2O, **S-16**-H_2O, **S-17**-H_2O about 103 kcal/mol at the B3LYP/LanL2DZ level; see Table S1 of the Supporting Information).

reference system, that is, the energy of **3** + **5a** + H_2O. The relative energy of water-free intermediates and TSs is evaluated by including the energy of a free water molecule (e.g., E_{rel} of **I-12** actually is E_{rel} of **I-12** + H_2O). E_{rel} of monoperoxo derivatives includes the energy difference between H_2O_2 and H_2O.

Activation energies ($\Delta E^{\ddagger}$) are referred to the corresponding reactants or intermediates and describe the activation energy involved only in the epoxidation step.

Results and Discussion

For the sake of comparison in Scheme 2 we report the front-spiro TS **8** for the reaction of ethene with complex **3**. Scheme 2 also illustrates the dihedral angles α and β that we use to describe the "spiro" character of TSs. α is the angle between the forming oxirane plane and the plane defined by Re and the reacting peroxo moiety (**A**, Scheme 2); β is the angle between the latter plane and the mean[36] double bond plane (**B**, Scheme 2). The ideal spiro orientation, $\alpha = \beta = 90°$, is never achieved, even with the symmetric and sterically free ethene double bond ($\alpha = 71°$, $\beta = 98°$ for TS **8**; Scheme 2). A deviation of α from 90° is the result of a rotation of the reacting peroxo−Re (ReO_4O_5) plane around the breaking O_4-O_5 bond (for the designation of the various atoms see Scheme 2 and Figures 2−7), while a deviation of β from 90° reflects tilting of that same plane with respect to the double bond plane. $\alpha < 90°$ indicates that there is, with respect to a perfect spiro orientation, a slight rotation of the ReO_4O_5 plane that moves the oxo side of the complex closer to the double bond C−C axis, while a widening of β (>90°) results from inclination of the ReO_4O_5 plane toward the double bond plane on the side of the nonreacting peroxo moiety.

TS **8** also demonstrates that there is an intrinsic asynchronicity (by 0.13 Å) of the forming bonds in the attack of **3** to a C=C double bond with the incipient bond on the side of the oxo group longer than that on the side of the peroxo group.

In our computational study we investigated the three mechanisms mentioned in the Introduction, that is, those which appeared the most reasonable ones for explaining the possible role played by the hydroxy functionality in driving the attack of the Re−peroxo complex to the double bond of allylic alcohols.

We assume that all equilibria involving Re complexes **2** and **3** as well as their hydrated forms **2**-H_2O and **3**-H_2O are established very rapidly, and consequently, competition between reaction routes, starting from the different complexes, can be discussed on the basis of the relative stability of the corresponding TSs without any explicit reference to the reactant equilibrium composition (Curtin−Hammett principle).[37]

Intermediates Derived from Alcohol Coordination and Corresponding Transition Structures. It is quite evident that we arrive at the intermediate complex **I-12** (Figure 2) if we replace the water molecule of **3**-H_2O by propenol (Figure 1) as axial donor. The Re−OHR distance in **I-12** is very similar (∼2.5 Å) to the Re−OH_2 distance in **3**-H_2O, and the formation of **I-12** from **3**-H_2O is calculated to be only slightly endothermic, by 0.6 kcal/mol (Table 1). Consequently, in the propenol reaction these two species are likely to be involved in a fast equilibrium in which both are present in significant amounts as entropic factors should not discriminate between them.

Alcohol coordination can take place also in an equatorial position, without water extrusion, to give **I-13**-H_2O (Figure 2) in a slightly exothermic process, by −1.3 kcal/mol. The Re−OHR distance is quite long, ∼3.2 Å, indicating a very weak interaction. The equilibrium between **I-13**-H_2O and **3**-H_2O should lie heavily on the side of the latter because the small enthalpy favoring the former complex is certainly overridden by a strong counteracting entropy.

Starting from the two intermediates **I-12** and **I-13**-H_2O, we managed to locate the corresponding first-order saddle points, **S-12** and **S-13**-H_2O, respectively (see Figure 2).

The high activation energy of the water-free axially coordinated **S-12** (Table 1) is most probably a consequence of the strain arising from structural distortion necessary to reach a spiro-like disposition of the reacting centers while keeping the coordination distance almost unaltered (Re−OHR = 2.6 Å). TS **S-12** also suffers from a noticeable tilting of the peroxo−Re plane ($\beta = 121°$). *This intramolecular reaction can be discarded as a productive epoxidation pathway since TS* ***S-12*** *has an energy (*E_{rel}*, Table 1) considerably larger than those of hydrogen-bonded TSs* ***20*****−****28*** *derived from* ***3*** *(water-free, Table 3*).

In TS **S-13**-H_2O with equatorially coordinated alcohol, the Re−OHR distance is considerably enhanced (3.8 Å), even longer than in complex **I-13**-H_2O (Figure 2). This reaction looks like an intermolecular epoxidation only slightly assisted by coordination of OH to Re. The propenol double bond and the reacting peroxo moiety succeed in adopting a satisfying spiro arrangement as judged from the angles $\alpha = 73°$ and $\beta = 88°$. The relative energy, E_{rel}, of **S-13**-H_2O is by 9.2 kcal/mol lower than that of **S-12**, and this stabilization can be attributed, in large part, to the coordination energy of the axial water. Note, however, that coordination induces relevant entropic costs so that at the free energy level the stability difference of these two TSs is strongly reduced, to 1.4 kcal/mol, if one applies the corresponding entropy, T[S(**S-12** + H_2O) − S(**S-13**-H_2O)] = 5.7 kcal/mol, and enthalpy (2.1 kcal/mol) corrections[38,39] as estimated from LANL2DZ frequencies. More relevant to our

(36) The mean double bond plane (for the two C atoms of the double dond and the four atoms bonded to them) was obtained according to the procedure described in: Cremer, D.; Pople, J. A. *J. Am. Chem. Soc.* **1975**, *97*, 1354.

(37) Seeman, J. I. *Chem. Rev.* **1983**, *83*, 83.

(38) Gas-phase entropies, standard state of molar concentration (ideal mixture at 1 mol/L and 1 bar).

(39) The difference in enthalpy between unsolvated derivatives and their solvated counterparts, either in the case of starting Re complexes (e.g., **3** vs **3**-H_2O) or of epoxidation TS (e.g., **22** vs **22**-H_2O), is by 2 kcal/mol smaller than the corresponding electronic energy difference. Note that basis set superposition error certainly favors hydrated forms with respect to related unsolvated derivatives. Moreover, it is quite obvious that hydrated complexes and TSs benefit from large water concentration.

Table 2. Bond Lengths (Å), Dihedral Angles (deg), OH-Stretching Frequencies (ν_{OH}, cm^{-1}), Net Atomic Charges (e) for Rhenium Bis(peroxo) Complexes **3** and **3**-H_2O and TSs for Propene (**18**) and Propenol (**20**−**28**) Epoxidation with the Re−bis(peroxo) Complex **3**, Charge Transfer from the Substrate for TSs **18** and **20**−**28** (in e)[a,b]

	3	**3**-H_2O	**18**	**20**	**21**	**22**	**23**	**24**	**25**	**26**	**27**	**28**
C_2-C_3	-	-	1.359	1.359	1.358	1.357	1.356	1.357	1.358	1.358	1.357	1.353
O_4-O_5	1.453	1.451	1.796	1.801	1.794	1.790	1.788	1.790	1.806	1.798	1.777	1.775
$Re-O_4$	1.946	1.962	2.011	2.024	2.013	2.011	2.030	2.011	2.018	2.005	2.010	2.017
$Re-O_5$	1.919	1.935	1.831	1.827	1.837	1.835	1.832	1.835	1.823	1.829	1.829	1.827
$OC_1C_2C_3$	-	-	-	123.2	134.5	15.6	129.7	13.5	−1.4	−3.8	145.1	6.9
HOC_1C_2	-	-	-	−65.0	−58.1	62.4	−57.8	60.2	−73.1	77.6	−72.6	87.8
ν_{OH}[c]	-	-	-	3674	3662	3657	3661	3650	3593	3614	3653	3662
atomic charges[d,e]												
O_4	−0.37	−0.40	−0.52	−0.53	−0.55	−0.56	−0.55	−0.55	−0.53	−0.51	−0.51	−0.51
O_5	−0.35	−0.36	−0.49	−0.48	−0.49	−0.48	−0.48	−0.48	−0.47	−0.47	−0.46	−0.46
O_6	−0.35	−0.36	−0.39	−0.39	−0.39	−0.39	−0.38	−0.39	−0.43	−0.43	−0.38	−0.36
O_7	−0.37	−0.40	−0.36	−0.36	−0.36	−0.36	−0.35	−0.36	−0.36	−0.35	−0.35	−0.35
O_8	−0.49	−0.44	−0.52	−0.52	−0.52	−0.51	−0.51	−0.51	−0.51	−0.52	−0.56	−0.58
charge transfer[e]	-	-	−0.36	−0.34	−0.35	−0.35	−0.34	−0.35	−0.36	−0.35	−0.33	−0.33

[a] Geometry data from B3LYP/IIb calculations. See also Table S2. [b] For the numbering see Figures 4,5. [c] Frequencies (wavenumbers) at the B3LYP/LanL2DZ level. Propenol conformer **5a**: $\nu_{OH} = 3678\ cm^{-1}$. [d] NBO charges from B3LYP/III′b//B3LYP/IIb. [e] Charge transfer from propene or propenol to the Re complex.

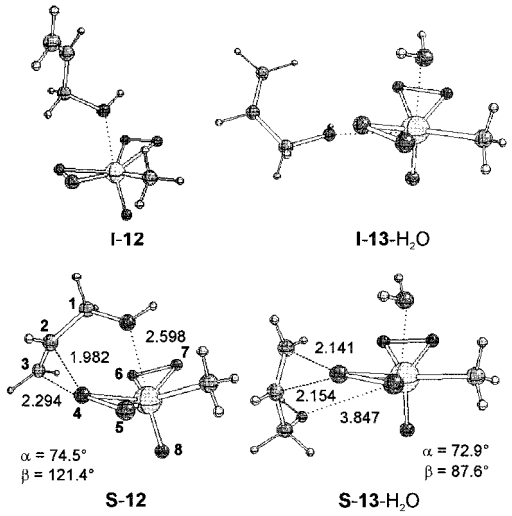

Figure 2. Optimized (B3LYP/IIb) intermediates derived from alcohol coordination **I-12**−**I-13**-H_2O and corresponding transition structures **S-12**−**S-13**-H_2O for the epoxidation of propenol **5** by the Re−bis(peroxo) complex **3**. Bond lengths in Å, angles in degrees.

discussion is the fact that E_{rel} of TS **S-13**-H_2O is notably higher (more than 4.5 kcal/mol) than that of several hydrated hydrogen-bonded TSs originating from **3**-H_2O (i.e., **21**-H_2O − **28**-H_2O, Table 4).

In summary, *calculations suggest that reaction channels starting from propenol coordinated complexes **I-12** and **I-13**-H_2O via transition structures **S-12** and **S-13**-H_2O represent feasible but not competitive entries to epoxidation pathways in accord with qualitative propositions by Espenson et al.*[24]

Metal−Alcoholate Intermediates and Related Transition Structures. The metal−alcoholate mechanism is well established for allylic alcohol epoxidations in the presence of Ti and V epoxidation catalysts[40−42] and can, in principle, be a viable pathway also for Re catalysis. In fact, allylic alcohols can add (at least formally) to either an oxo−Re or peroxo−Re moiety of, for example, complexes **3** and **3**-H_2O in a process, indicated as metal−alcoholate binding, that gives rise to metal−alcoholate intermediates.

Table 3. Relative Energies (E_{rel}) and Activation Barriers ($\Delta E^{\ddagger}$) of TSs for the Reactions of Bis(peroxo) **3** with Propene (**18** and **19**) and Propenol (**20**−**28**)[a,b]

	type of approach and conformation	O_4-O_5/ O_6/O_8[c]	$E_{rel}(\Delta E^{\ddagger})$[d] kcal/mol	$E_{rel}(\Delta E^{\ddagger})$[e] kcal/mol
3 + **5a** + H_2O	-	-	0.0	0.0
18	exo,trans	-	(10.1)	-
19	endo,cis	-	(10.9)	-
20	anti,exo,trans,out	no hb	12.2	11.9
21	syn,exo,cis,out	O_4-O_5	9.4	8.6
22	syn,exo,cis,in	O_4-O_5	8.8	7.8
23	syn,exo,trans,out	O_4-O_5	9.6	8.8
24	syn,exo,trans,in	O_4-O_5	9.0	7.6
25	syn,endo,cis,in	O_6	9.2	7.8
26	syn,endo,trans,in	O_6	10.3	8.8
27	syn,endo,trans,out	O_8	10.8	10.8
28	syn,endo,trans,in	O_8	10.4	8.8

[a] For TSs **20**−**28** E_{rel} coincides with $\Delta E^{\ddagger}$. E_{rel} (including the energy of a free water molecule) calculated with respect to the sum of the reactant energies **3** + **5a** + H_2O. [b] ZPE values (B3LYP/LanL2DZ) of TS-**20**−**28** are very similar (∼86 kcal/mol, Table S3). [c] Oxygen centers involved in hydrogen bonding. [d] B3LYP/III′b//B3LYP/IIb calculations. For reactant energies (**3** + **5a** + H_2O) see footnote b of Table 1. Propene **4**: $E = -117.945575$ hartree. [e] B3LYP/IIIb//B3LYP/IIb calculations. Reactant energies: E(**3**) = −495.153808 hartree, E(**5a**) = −193.17540 hartree, and $E(H_2O) = -76.447448$.

In the case of alcohol addition to bis(peroxo) complexes we located four local minima corresponding to unsolvated, **I-14** and **I-15**, and hydrated, **I-16**-H_2O and **I-17**-H_2O, intermediates (Figure 3). **I-14** and **I-15** derive from attachment of the alcoholate moiety in the axial position of **3** with concomitant H^+ transfer to an oxo or peroxo oxygen, respectively. In the case of **I-16**-H_2O and **I-17**-H_2O the alcoholate enters at the equatorial position of **3**-H_2O, opposite to the methyl group, while the aquo ligand continues to occupy the axial position of the complex. Once again the proton is transferred to an oxo and peroxo oxygen, respectively.

Addition of a proton to the oxo functionality with formation of intermediates **I-14** and **I-16**-H_2O, which contain two peroxo moieties, is thermodynamically disfavored over proton addition to the peroxo moiety, leading to **I-15** and **I-17**-H_2O with both a peroxo and a hydroperoxo system. Moreover, the latter two intermediates differ from each other in an important characteristic. In **I-15**, with the alcoholate in axial position, the OOH moiety is coordinated in a bidentate fashion (with a covalent

(40) Hoveyda, A. H.; Evans, D. A.; Fu, G. C. *Chem. Rev.* **1993**, 1307.
(41) (a) Sharpless, K. B.; Michaelson, R. C. *J. Am. Chem. Soc.* **1973**, *95*, 6136. (b) Rossiter, B. E.; Verhoeven, T. R.; Sharpless, R. B. *Tetrahedron Lett.* **1979**, *49*, 4733.
(42) (a) Jørgensen, K. A.; Wheeler, R. A.; Hoffmann, R. *J. Am. Chem. Soc.* **1987**, *109*, 3240. (b) Wu, Y.; Lai, D. K. *J. Org. Chem.* **1995**, *60*, 673. (c) Wu, Y.; Lai, D. K. *J. Am. Chem. Soc.* **1995**, *117*, 11327.

Table 4. Relative Energies (E_{rel}) and Activation Barriers ($\Delta E^{\ddagger}$) for TSs of the Reaction of the Bis(peroxo) Complex **3**-H_2O with Propenol[a,b]

	type of approach and conformation	O_4-O_5/ O_6/O_8[c]	E_{rel}[a,d] kcal/mol	$\Delta E^{\ddagger}$[a,d] kcal/mol	E_{rel}[a,e] kcal/mol	$\Delta E^{\ddagger}$[a,e] kcal/mol
3 + **5a** + H_2O	-	-	0.0	-	0.0	-
3-H_2O + **5a**	-	-	−12.0	0.0	−16.4	0.0
21-H_2O	syn,exo,cis,out	O_4-O_5	−1.6	10.4	−8.9	7.5
22-H_2O	syn,exo,cis,in	O_4-O_5	1.5	13.5	−4.5	11.9
24-H_2O	syn,exo,trans,in	O_4-O_5	0.5	12.5	−5.6	10.8
25-H_2O	syn,endo,cis,in	O_6	2.2	14.2	−2.6	13.8
28H_2O	syn,endo,trans,in	O_8	4.4	16.4	−1.3	15.1

[a] E_{rel} are referred to **3** + **5a** + H_2O and $\Delta E^{\ddagger}$ to **3**-H_2O + **5a**. [b] ZPE values (B3LYP/LanL2DZ) of TSs **21**-H_2O−**28**-H_2O are very similar (~102 kcal/mol, Table S4). [c] Oxygen centers involved in hydrogen bonding. [d] B3LYP/III′b//B3LYP/IIb calculations. For reactant absolute energies see footnote b of Table 1. [e] B3LYP/IIIb//B3LYP/IIb calculations. For reactant absolute energies see footnote e of Table 3.

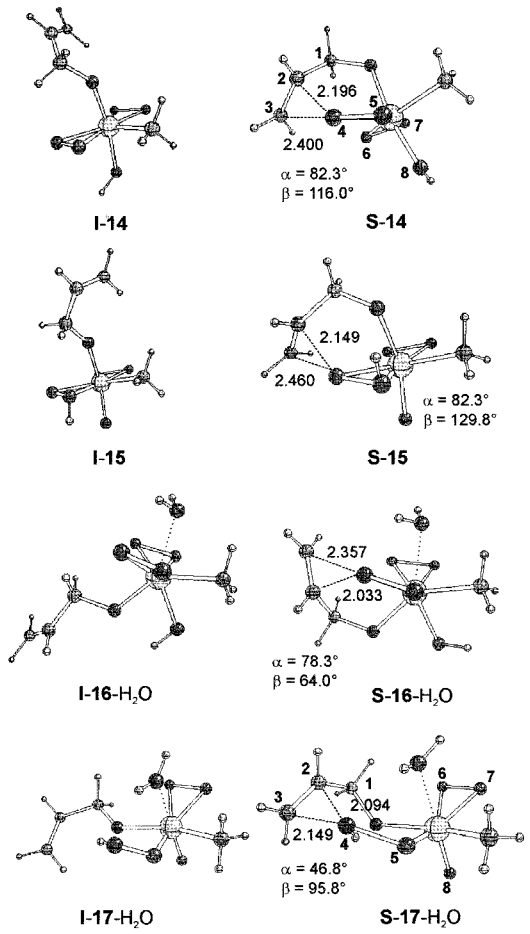

Figure 3. Optimized (B3LYP/IIb) metal−alcoholate intermediates **I-14**−**I-17**-H_2O and corresponding transition structures **S-14**−**S-17**-H_2O for the epoxidation of propenol **5** by the Re−bis(peroxo) complex **3**. Bond lengths in Å, angles in degrees.

metal−oxygen bond and a further weaker coordinative bond), while in **I-17**-H_2O, with the alcoholate equatorially coordinated, the hydroperoxo group features one-end coordination (see Figure 3).

Three out of these four intermediates are high-energy intermediates (cf. E_{rel}; Table 1). Only the hydroperoxo **I-17**-H_2O (with the alcoholate in equatorial position) is lower in energy (by 6.2 kcal/mol) than the reactants and seems to have some chance to be competitive in the epoxidation reaction.

However, location of transition structures showed that this is not the case. In fact, intramolecular epoxidation in **I-17**-H_2O can take place only via saddle point **S-17**-H_2O in which the β-oxygen of the hydroperoxo group is involved. As mentioned in the Introduction, hydroperoxo systems are less efficient as epoxidant than peroxo groups, and hydroperoxo β-oxygen is less reactive than α-oxygen.[7,9] Thus, the relatively stable **I-17**-H_2O is forced to go to the epoxide via the high-energy saddle point **S-17**-H_2O losing most of the energy advantage it has at the starting point. TS **S-17**-H_2O still exhibits the lowest energy compared to the other possible metal−alcoholate competitors; however, its energy is very similar to that of TS **S-15.** The latter TS benefits from the possibility to react at the hydroperoxo α-oxygen and should also be favored, relative to the former, by entropic factors. Both of these TSs are significantly distorted with respect to the ideal spiro geometry.

Reaction routes through TSs **S-14** and **S-16**-H_2O are even more difficult than those via **S-15** and **S-17**-H_2O. This statement is based not only on the large amount of energy necessary for forming the intermediate, but also on the remarkably large activation energies, >20 kcal/mol, required for the subsequent intramolecular epoxidation (Table 1). The low reactivity of **I-14** and **I-16**-H_2O stems from severe angle strain necessary to achieve spiro-like TSs. Moreover, the large tilting of the Re−peroxo plane exhibited by **S-14** (β = 116°) and **S-16**-H_2O (β = 64°), indicates that the orientation of π(C=C) and σ^*(O−O) is quite different from that required for an efficient interaction.

Whatever the underlying reason of the above observations—high energy of intermediates and large activation energies for intramolecular epoxidation via TSs that are much less stable (by >15 kcal/mol, Table 1) than solvated or unsolvated hydrogen bonded TSs,—*these results provide convincing evidence that alcoholate−metal complexes do not contribute to product formation and can be confidently neglected when discussing Re−peroxo-catalyzed epoxidations of allylic alcohols.* Our calculations confirm the previous conclusion by Adam et al. on the basis of experimental data.[12,14]

In light of these data we refrained from performing a complete search for TSs starting from metal−alcoholate complexes. In particular, we did not investigate possible metal−alcoholate complexes derived from monoperoxo complexes.

As for a comparison among epoxidations catalyzed by different transition metal complexes we emphasize the striking contrast between Ti- and V-catalyzed reactions[40−42] in which the metal−alcoholate bond drives the allylic OH directivity while this mechanism, although viable, is energetically completely out-of-reach for the corresponding Re-catalyzed reactions. On the other hand, we recall that the formation of an alcoholate intermediate was also rejected for epoxidations of allylic alcohols with Mo− and W−peroxo complexes while hydrogen bonding (between OH and the reacting peroxo fragment) was considered consistent with kinetic data.[43]

Hydrogen-Bonded Transition Structures for the Reaction of Monoperoxo− and Bis(peroxo)−Re Complexes. Propenol Conformers. To discuss hydrogen-bonded transition structures

(43) Arcoria, A.; Ballistreri, F.; Tomaselli, G.; DiFuria F.; Modena, G. *J. Org. Chem.* **1986**, *51*, 2374.

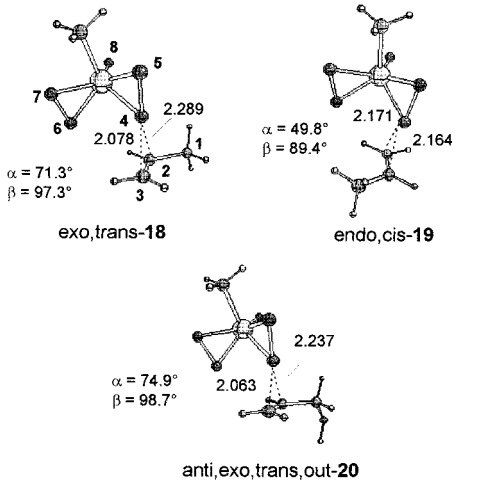

Figure 4. Optimized (B3LYP/IIb) transition structures for the epoxidation of propene (**18**, **19**) and propenol (**20**) in anti fashion by the unsolvated Re−bis(peroxo) complex **3**. Bond lengths in Å, angles in degrees.

it is useful to start from the propenol conformers (Figure 1). The two most stable, out-**5a** and in-**5b**, out of the five fast equilibrating conformers,[18] have similar energy. Conformer out-**5a** features eclipsing between the inside C-H bond and the double bond while the OH group resides in an "outside" position. The OH group of in-**5b** occupies the "inside" position and the C−O bond approximately eclipses the C═C bond. In both conformers the hydroxyl group is properly oriented to be easily involved in hydrogen bonding with the oxygen centers of the attacking peroxo rhenium complex. Actually, the CH_2-OH conformation in hydrogen-bonded syn TSs more or less closely resembles that of out-**5a** or in-**5b** and, accordingly, TSs are given the descriptor out and in, respectively.

Strategy for TS Search and TS Nomenclature. In Figure 4, we compare two front-spiro TSs for propene (**4**) epoxidation and one anti TS for propenol (**5**) epoxidation. The former TSs are free from both hydrogen bonding and inductive effects, while in the latter the electron-attracting effect of the OH group is not obscured by hydrogen bonding.

A complete investigation of all possible syn hydrogen-bonded TSs for the propenol epoxidation with **2**, **2**-H_2O, **3,** and **3**-H_2O (also considering the conformational freedom of the CH_2OH group) would have been unmanageably complicated, too expensive, and probably useless. Consequently, we chose to investigate all syn pathways involving the bis(peroxo) complexes **3** and **3**-H_2O that are meaningful for a reliable evaluation of hydrogen-bonding interaction in the reaction under study.

For the reaction of **3** with propenol we located nine (hopefully all) "front-spiro" TSs where the "front" peroxo oxygen is transferred, that is, the peroxo oxygen distal to the methyl group (Figure 5 and Table 3). We neglected "back-spiro" TSs which involve the peroxo oxygen proximal to the methyl group because previous studies on ethene epoxidation have shown that the latter TSs lie much higher in energy (by >6 kcal/mol) than the corresponding "front-spiro" TSs.[7,9] Then we extended our study to epoxidation with **3**-H_2O by locating five syn TSs with an axial water ligand (Figure 6 and Table 4) which correspond to the most stable TSs that are derived from the unsolvated complex **3**.

We anticipated that bis(peroxo) complexes should be at least as reactive as (but most probably more reactive than) the monoperoxo complexes **2** and **2**-H_2O. The computational results (see below) confirmed this hypothesis, thus justifying the

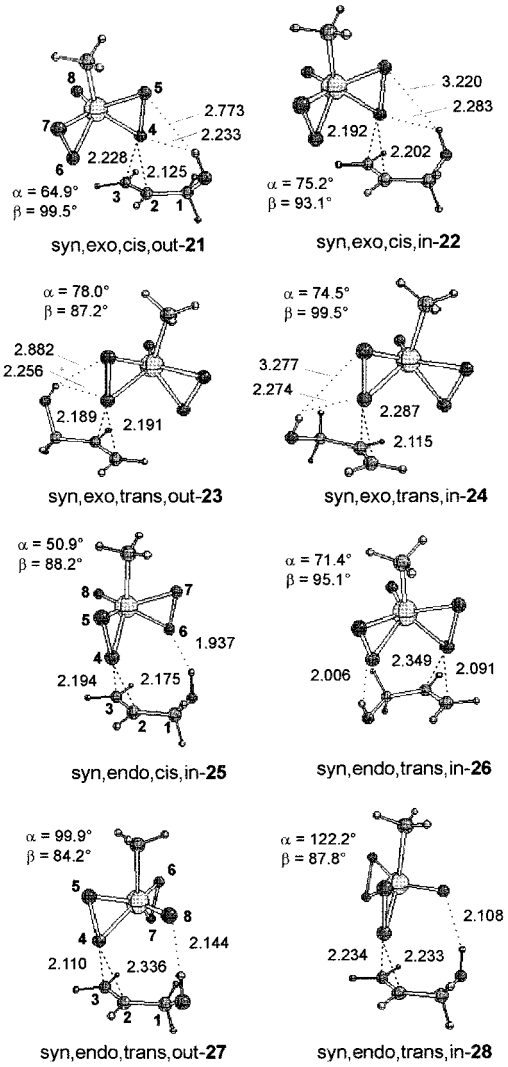

Figure 5. Optimized (B3LYP/IIb) syn transition structures **21**-**28** for the epoxidation of propenol **5** by the unsolvated Re−bis(peroxo) complex **3**. Bond lengths in Å, angles in degrees.

limitation of the TS search to a few examples of the latter complexes. The presence of only one peroxo bridge in **2** strongly reduces the number of possible epoxidation TSs. We consider characterization of three unsolvated TSs (two syn "front-spiro" and one syn "back-spiro" TS) and two back-spiro hydrated TSs sufficient for providing a clue on the role of complexes **2** in propenol oxidation.

In addition to conformational descriptors (in and out), the following descriptors are given to TSs in order to convey as clearly as possible the orientation of the attacking peroxo complex:

(i) as for facial selectivity (i.e., selectivity of attack to the two diastereotopic faces of the double bond of out-**5a** and in-**5b**) a transition structure is classified as syn if the attacking Re−peroxo complex lies on the side of the OH bond and anti if it lies on the opposite side;

(ii) the descriptors endo and exo indicate that, with respect to the plane of the forming oxirane ring, the Re atom (and its substituents) lies on the same and opposite side, respectively, of the CH_2OH group;

(iii) the "non-reacting" peroxo group can lie, with respect to the plane of the reacting Re−peroxo moiety, on the same or opposite side of the ═$CHCH_2OH$ part of the allylic alcohol. These two TSs are designated as cis and trans, respectively.

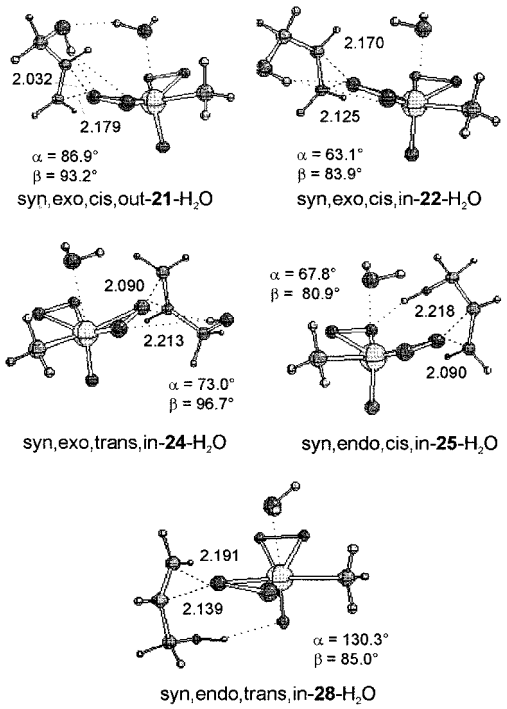

Figure 6. Optimized (B3LYP/IIb) syn transition structures for the epoxidation of propenol **5** by the hydrated Re−bis(peroxo) complex **3**-H_2O. Bond lengths in Å, angles in degrees.

Transition Structures for the Reaction of Unsolvated 3 with Propene and for an anti Attack of 3 on Propenol. The most (exo,trans-**18**) and the last (endo,cis-**19**) stable TS out of the four TSs,[44] located by us for the reaction of **3** with propene, are reported in Figure 4 (see also Table 2).

The geometry of transition structure **18** is almost identical to that of TS **8** for the reaction of **3** with ethene, but more asynchronous with the two C−O bonds differing by 0.21 Å. Note in particular how in both TSs the forming oxirane plane is symmetrically located with respect to the two sides of the double bond. Some structural aspects of TS **18** are common to all TSs, for example, (i) a very small elongation of the C_2-C_3 bond (by 0.02 Å), (ii) a substantial elongation of the peroxo bond O_4-O_5 (by 0.34 Å), and (iii) the fact that the $Re-O_4$ bond is elongated less (by 0.06 Å) than the $Re-O_5$ bond is shortened (by 0.09 Å) (e.g., TSs of Table 2).

The sterically very congested TS **19** nicely illustrates how the attacking bis(peroxo)−Re complex can adjust the approach trajectory to accommodate and lessen steric crowding at the TS. Noteworthy are (i) a lengthening of the forming bond adjacent to the methyl group (this renders bond formation almost synchronous), (ii) an inclination of the forming oxirane plane to the opposite side of the methyl group, (iii) a rotation of the complex around the O_4-O_5 bond with a large reduction of the angle α. All these variations (also β deviates by 8° from the ideal value) take place at a low energy cost (**19** is only 0.8 kcal/mol higher than **18**), thus demonstrating the flexibility of the TS geometry of these reactions.

The average incipient bond length in the TSs of peroxo−Re complex epoxidation is only slightly longer (∼0.1 Å) than that in TSs of dimethyldioxirane epoxidations[20b,21] and the two epoxidants are expected to exhibit similar sensitivity to steric effects. In fact, the energy difference between endo and exo TSs for dimethyldioxirane epoxidation of propene (0.63 kcal/mol at the B3LYP/6-31G* level)[20b] is quite close to that between endo and exo TSs for bis(peroxo)−Re epoxidation (≤0.8 kcal/mol) of the same alkene (Table 3 and ref 43).

Another important aspect that testifies the electrophilic nature of attack by **3** to propene is the noticeable transfer of electronic charge from the alkene to the complex (−0.36 e) which is slightly larger than that from propene to dimethyldioxirane (−0.30 e).[20] It is interesting to note that electronic charge is mostly transferred, as expected, to the reacting peroxo moiety (O_4-O_5) but, somewhat surprisingly, to a similar extent to the attacking O_4 and to O_5. For example, on going from **3** to TS **18**, the charge of O_4, changes by −0.15 e and that of O_5 by −0.14 e (Table 2). This observation stands in striking contrast to the findings for the dioxirane reaction[20b,21] where the net negative charge on the attacking oxygen does not change appreciably, while that of the other oxygen, farther from the double bond, increases by −0.20 e. The latter charge distribution better conforms to the generally accepted view that these reactions can be described as a nucleophilic S_N2 attack, by the π bond on the O−O system, with "heterolytic" breaking of the O−O bond at the beginning of the process.

Introduction of an electron-attracting OH group in anti position of TS **18**, that is, on passing from **18** to TS anti,exo,-trans,out-**20**, does not give rise to relevant geometry changes and, for example, only slightly reduces the asynchronicity of the incipient bond (Figure 4). Given the electrophilic nature of the attack by the Re complex on the double bond, one anticipates that the electron-withdrawing inductive effect of the OH group reduces the electron transfer in **20** as compared to **18**. Actually, the predicted transfer of electronic charge from olefin to peroxo complex (−0.36 and −0.35 e for transition structures **18** and **20,** respectively) is, as expected, smaller in the propenol than in the propene reaction, but the difference is negligible.

However, the expected rate retarding effect of the OH group emerges clearly in the enhancement of calculated activation energies (Table 3) on passing from the propene reaction ($\Delta E^{\ddagger}$ = 10.1 kcal/mol for TS **18**) to the anti attack on propenol ($\Delta E^{\ddagger}$ = 12.2 kcal/mol for TS **20**). A similar observation has already been reported for calculated activation energies of propene vs propenol epoxidations with both dioxiranes[21] and peroxyformic acid.[18b]

Hydrogen Bonding in syn TSs for the Reaction of Unsolvated Re−Bis(peroxo) Complex 3 with Propenol. A stabilizing hydrogen-bonding interaction is present in all syn transition structures located by us for attack of the "front oxygen" of **3** on propenol. In fact, all syn TSs **21**−**28** (Figure 5) are more stable (at the IIIb and III′b levels by 1.1−4.3 and 1.4−3.4 kcal/mol, respectively) than anti,exo-**20** and some of them even show a definitely lower activation energy as compared to that of the corresponding propene TSs. Thus, hydrogen bonding favors syn TSs by some kcal/mol with respect to the anti TS. Moreover, consistently with the presence of a hydrogen bond, the OH-stretching frequencies (Table 2) are notably lower in syn TSs (by 15 to 90 cm^{-1} with the strongest reduction for **25** and **26**) as compared to those of the corresponding propenol conformers (**5a** for out TSs and **5b** for in TSs). On the other hand, the OH-stretching frequency of anti,exo-**20** (3674 cm^{-1}) does not appreciably deviate (3678 cm^{-1}) from that of **5a**.

Figure 5 shows that both hydrogen-bonding models advanced by experimentalists, represent viable reaction channels, but also

(44) For the reaction of the Re−bis(peroxo) complex **3** with propene **4** only "front" attacks (see ref 7) were considered. The energies (III′b/IIb), the incipient bond lengths and the α and β angles (IIb) of the other two TSs are as follows: exo,cis TS, E = −613.095355 hartree, C_1-O_4 = 2.185 Å, C_2-O_4 = 2.161 Å, α = 71.1°, β = 94.4°; endo,trans TS, E = −613.094712 hartree, C_1-O_4 = 2.072 Å, C_2-C_4 = 2.325 Å, α = 78.2°, β = 99.1°.

that several other transition structures can be operative on the way to final epoxides.

There are four TSs, **21**−**24**, in which OH forms a hydrogen bond to oxygen centers of the reacting peroxo moiety. Two of them have the OH group in outside position ($OC_1C_2C_3 = 134°$ and 130° for **21** and **23**, respectively) and are similar to the qualitative transition structures advanced by Adam et al.[12,14] The other two TSs exhibit an OH group in inside conformation ($OC_1C_2C_3 = 16°$ and 13° for **22** and **24**, respectively). Previously,[12,14] this conformation was not considered, probably because it does not permit efficient hydrogen bonding with O_5. In our opinion, the most reasonable description of the hydrogen bonds in TSs **21**−**24** is that of "bridged" hydrogen bonds involving, to some extent, both peroxo oxygens (in particular in **21** and **23** while in **22** and **24** O_4 seems to be favored). In syn TSs **21**−**24**, concomitant with the presence of hydrogen bonding, there is a slight enhancement of the negative charge on O_5 in comparison to the anti TS **20** (Table 2).

In accord with Espenson's proposal[24] there are also TSs with hydrogen bonding to the nonreacting peroxo moiety (O_6-O_7) as documented by TS **25** and TS **26**, both having OH in inside conformation ($OC_1C_2C_3 = -1°$ and −4° for **25** and **26**, respectively). As judged by the strong reductions in the OH stretching frequencies and the relatively short $OH-O_6$ distances, these two TSs have the strongest hydrogen bonds and hydrogen bonding seems to favor O_6, which is also more negatively charged than O_7 (Table 2).

Finally, given that the O_8 center exhibits the largest net negative charge, it does not come as a surprise that also this oxo oxygen can act as hydrogen bond acceptor, as shown in TS **27** (OH in outside conformation) and TS **28** (OH in inside conformation).

As for the approach geometry of the reactants, the need to adopt a disposition favorable for hydrogen bonding drives the distortion from the ideal orientation present in TSs **18** or **20**. For example, it is quite evident that the largest variations of the parameter α observed in **25** and **28** (α = 51° and 122°, respectively, as compared to 71° and 75° in **18** and **20**) can be easily rationalized as the result of a rotation of the Re complex fragment around the O_4-O_5 bond, necessary to guarantee favorable alignment and distance to the moieties O_6-H-O and O_8-H-O, respectively. It is important to stress a common structural feature of all TSs **21**−**28**: as far as the orientation of the ReO_4O_5 ring with respect to the C=C bond axis or to the plane of the oxirane being forming are concerned, *all of these TSs have to be classified as "spiro-like"; none can be designated as essentially "planar" TS.*

Thus, *one can conclude that TSs for alkene and allylic alcohols epoxidations with peroxy acids, dioxiranes, and Re−peroxo complexes share the feature of a spiro geometry in which the plane of the attacking peroxo (peroxy) moiety is oriented almost perpendicularly to the plane of the oxirane under formation.*

The relative energies for the eight TSs **21**−**28** are reported in Table 3. The trend obtained at the level IIIb does not change significantly on passing to the higher level III′b (with diffuse functions added to main group atoms), even if the latter method predicts larger activation energies (on average by about 1 kcal/mol). All TSs lie in a range of 2 kcal/mol, bracketed by TS syn,exo,cis,in-**22** as the most stable TS and by TS syn,endo,-trans,out-**27** as the least stable TS. From the point of view of a qualitative analysis, it is disappointing that we were unable to identify any structural characteristic that might definitely favor or disfavor one TS with respect to the others. Would the reaction occur via unsolvated TSs, all eight TSs should contribute to the formation of the final epoxide, with most of them engaged in a balanced competition.

However, TSs with hydrogen bonding to the reacting peroxo system are preferable over TSs with hydrogen bonding to the nonreacting peroxo system while TSs hydrogen-bonded to the oxo oxygen follow with a small energy difference.

We have already commented on the rate retardation caused by the electron-attracting inductive effect of the OH group in case of an anti attack of **3** to propenol. This factor is obviously present also in syn TSs but here it is offset by stabilization due to hydrogen bonding. Actually, the activation energy of several syn TSs for the propenol reaction is lower than that of TS **18** for the propene reaction. On this basis, propenol should be epoxidized faster than propene, in contrast with experimental observations; for example, 2-cyclohexen-1-ol reacts 6 times more slowly than 3-methylcyclohexene.[24] In the case of dioxirane epoxidation of propenol[21] the very same discrepancy between experimental and theoretical data has been resolved by showing that the propene reaction is favored as compared to propenol reaction by entropic factors and, more strongly, by solvent effects. In contrast, in the case of Re−peroxo epoxidations calculated gas-phase entropic factors favor propenol (with $\Delta S^{\ddagger}$ values ranging from −36.7 to −40.8 eu) over propene reaction ($\Delta S^{\ddagger} = -41.2$ eu). Thus, the higher reactivity observed for the latter in condensed phase is most probably the result of solvent effects.

Transition Structures Originating from the Hydrated Re−Bis(peroxo) Complex 3-H_2O. Coordination of a water molecule to **3** gives **3**-H_2O for which calculations predict a large energy stabilization which, however, is basis set dependent: 12 and 16 kcal/mol (Table 4) for basis sets III′b and IIIb, respectively. The equilibrium between **3** and **3**-H_2O should lie on the side of the latter because the energy advantage of **3**-H_2O over **3** should be enough to offset the entropic cost, $T[S(\mathbf{3} + H_2O) - S(\mathbf{3}\text{-}H_2O)] = 9.0$ kcal/mol,[38,39] of its formation.

It is widely accepted that in the case of the Re−bis(peroxo) complex the actual epoxidizing species is a base adduct of the bis(peroxo) complex, for example, with a water molecule, **3**-H_2O.[4,6,12,14,24] Since water is always present in Re-catalyzed H_2O_2 epoxidations of olefins, it was mandatory to locate representative examples of transition structures originating from the attack by **3**-H_2O on propenol. Our choice was guided by TSs characterized for the reaction of **3**, and we managed to locate five hydrated TSs, **21**-H_2O, **22**-H_2O, **24**-H_2O, **25**-H_2O, and **28**-H_2O (Figure 6). Note, in particular, that three of them (**22**-H_2O, **25**-H_2O, and **28**-H_2O) correspond to the most stable water-free TSs, one for each kind of hydrogen-bonding interaction, that is, involving oxygen centers either of the reacting or of the nonreacting peroxo system as well as of the oxo function.

Water coordination takes place opposite to the oxo oxygen (Figure 6). The structural similarity between hydrated TSs and the corresponding water-free TSs is evident, even if the presence of water causes relevant geometry changes. One common feature of all hydrated TSs is that they exhibit average incipient bond lengths slightly shorter than those of related unsolvated TSs. As for the α and β angles, which define the "spiro" orientation, one notes that β is always slightly smaller in the solvated TSs than in their unsolvated counterparts, while α can be either much smaller or significantly larger. *All of these data once again emphasize the flexibility of TSs for Re−peroxo epoxidation, but the structures always remain in the range of a "spiro" geometry.*

For two TSs of Figure 6, remarks are in order: (i) in TS **24**-H_2O, water coordination occurs without altering the geometry

(i.e., α and *β*) of the corresponding TS **24**; (ii) in TS **21**-H_2O, the water molecule operates both as electron pair donor to the Re center and as hydrogen bond donor to the olefinic OH.

In light of these observations it is understandable that **21**-H_2O, stabilized by a further hydrogen bond, exhibits the lowest energy (E_{rel}) among the solvated TSs (Table 4) and that **24**-H_2O, apparently free from steric crowding, is the next most stable TS. Energy gaps between solvated TSs (see E_{rel} and $\Delta E^{\ddagger}$ in Table 4) are higher than those between unsolvated TSs (Table 3) so that hydration seems to definitely tip the balance in favor of TSs with hydrogen bonding to the reacting peroxo bridge (**21**-H_2O and **24**-H_2O), whereas those with hydrogen bonding to the oxo functionality (**28**-H_2O) are no longer competitive. Notice how the most stable hydrated TS **21**-H_2O features an outside conformation with the $OC_1C_2C_3$ dihedral angle, 124.9°, very close to that proposed by Adam et al. for their planar TS model (**C**, Scheme 4). On the other hand, in TS **24**-H_2O the OH group adopts an inside conformation, $OC_1C_2C_3 = 15.4°$.

The proposal by Espenson et al.[24] of a dominating TS, with hydrogen bonding to the nonreacting peroxo bridge (**G**, Scheme 4), for the Re−bis(peroxo)-catalyzed epoxidation of allylic alcohols is not supported by our calculations. Model **G** is certainly reasonable for qualitative TSs (as demonstrated by TSs **25**, **26**, and **25**-H_2O), but it is neither the only possible structure nor does it represent the dominant pathway to the final epoxide.

Hydration is strongly beneficial not only for the starting Re−bis(peroxo) complex but also for the related TSs. The effect for the starting complex is more pronounced than that for TSs; in fact, as for ethene epoxidation,[7,9] water coordination enhances the activation barriers (by 1−4 kcal/mol at the higher calculation level).

Notwithstanding this barrier increase, solvated TSs reside at much lower energies than their unsolvated counterparts (compare E_{rel} values in Tables 3 with those in Table 4). However, this energy difference is basis-set-dependent and decreases by 3.5−6.0 kcal/mol with the introduction of diffuse functions. Moreover, hydrated TSs are entropically disfavored (by ∼9 kcal/mol in the gas phase)[38,39] with respect to the corresponding water-free TSs. These observations prevent a definitive decision whether **3** or **3**-H_2O is the more active epoxidant species in solution. However, the latter complex should prevail in the precence of high water concentration.

Transition Structures for the Reactions of Re−Monoperoxo Complex 2 and Its Hydrated Form 2-H_2O. Just to have a clue on the reactivity of Re−monoperoxo complexes with propenol, we located the five TSs reported in Figure 7 and Table 5. All of them have a spiro geometry in which α and *β* are certainly influenced by hydrogen bonding. TS **30** corroborates the observation (cf. TS **28**) that an efficient hydrogen-bonding interaction can involve the oxo functionality in an endo TS. This becomes feasible by a sizable change of the angle α.

The energy gap between unsolvated TS **31** and its hydrated counterpart **31**-H_2O, 5.7 kcal/mol in favor of **31**-H_2O (Table 5), is overcompensated by a counterbalancing entropy gap. In fact, in the gas phase the entropy difference is estimated to about 9 kcal/mol in favor of **31**.[38,39] This observation suggests that unsolvated TSs outweigh their hydrated competitors in the epoxidation via monoperoxo complex.

As for the competition between monoperoxo and bis(peroxo) Re complexes, Espenson et al.[24] concluded that (i) the epoxidation rate of allylic alcohols by the Re−monoperoxo complex **2** was negligible in comparison with that by the Re−bis(peroxo) complex **3**-H_2O, and (ii) this observation is unique and does not hold for any other substrate studied thus far.

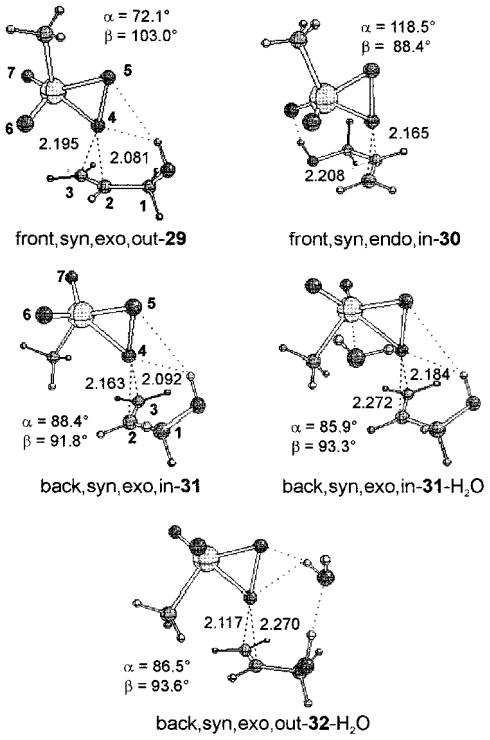

Figure 7. Optimized (B3LYP/IIb) front- and back-spiro transition structures **29**−**32** for the epoxidation of propenol **5** by the unsolvated Re−monoperoxo complex **2** and by the corresponding solvated complex **2**-H_2O. Bond lengths in Å, angles in degrees.

The three unsolvated TSs **29**−**31** as well as the hydrated TS **31**-H_2O arising from the monoperoxo complex **2** exhibit higher energies E_{rel} than those of the related TSs originating from Re−bis(peroxo) complexes. Thus, our calculations confirm the deduction from the experimental kinetics. Moreover, it should be stressed that the calculated difference in reactivity of the two hydrated Re−peroxo species **3**-H_2O and **2**-H_2O is larger for the epoxidation of propenol than for that of ethene,[7,9] and this finding is in agreement with the second remark by Espenson et al.[24]

TS **32**-H_2O deserves a brief comment (Figure 7). It was obtained as a result of attempts to locate, for the hydrated monoperoxo species, a TS in which the water molecule at the same time acts as base to Re and participates in the hydrogen bond to the OH group (cf. TS **21**-H_2O). TS **32**-H_2O opens the big and very complicated question of how intermolecular hydrogen bonding by water present in the reaction mixture (in general, specific and nonspecific solvation effects) can influence the role of TSs described above. These questions have to be left to future investigations.

Conclusions

For the epoxidation of propenol with rhenium complexes we explored, using B3LYP hybrid density functional calculations, the three mechanisms that appeared the most reasonable ones for rationalizing the possible role played by the hydroxy functionality in driving the attack by the Re−peroxo complex to the double bond of allylic alcohols, namely (i) coordination of propenol (as lone pair donor) to the rhenium complex, followed by intramolecular epoxidation, (ii) formation of a metal−alcoholate, derived from addition of propenol to the complex (either to the Re═O bond or to the three-membered ReOO peroxo ring) with formation of a metal−OR bond,

Table 5. Relative Energies (E_{rel}), Activation Barriers ($\Delta E^{\ddagger}$) for TSs of the Reaction of Monoperoxo Complexes **2** and **2**-H_2O with Propenol[a,b]

	type of approach and conformation	O_4-O_5/ O_6/O_8[c]	E_{rel}[a,d] kcal/mol	$\Delta E^{\ddagger}$[a,d] kcal/mol	E_{rel}[a,e] kcal/mol	$\Delta E^{\ddagger}$[a,e] kcal/mol
3 + **5a** + H_2O	-	-	0.0	-	0.0	-
2 + **5a** + H_2O	-	-	−3.4	0.0	−5.2	0.0
2-H_2O + **5a**	-	-	−7.7	0.0	−13.7	0.0
29	syn,exo,cis,out	O_4-O_5	12.3	15.7	9.3	14.5
30	syn,endo,cis,in	O_7	11.7	15.1	8.2	13.4
31	back,syn,exo,cis,in	O_4-O_5	11.6	15.0	8.0	13.2
31-H_2O	back,syn,exo,cis,in	O_4-O_5	5.9	13.6	−2.5	11.2
32-H_2O	back,syn,exo,cis,out	O_4-O_5	2.7	10.4	−3.9	9.8

[a] E_{rel} are referred to **3** + **5a** + H_2O. They include the energy difference between H_2O_2 and H_2O. $\Delta E^{\ddagger}$ for **29**−**31** are referred to **2** + **5a** and for **31**−H_2O and **32**-H_2O to **2**-H_2O + **5a**. [b] ZPE values (B3LYP/LanL2DZ) of TSs **29**−**31** as well as of **31**-H_2O and **32**-H_2O are very similar (about 85 and 100 kcal/mol, respectively, Table S5). [c] Oxygen centers involved in hydrogen bonding. [d] B3LYP/III′b//B3LYP/IIb calculations. For reactant absolute energies see footnote b of Table 1. [e] B3LYP/IIIb//B3LYP/IIb calculations. For reactant absolute energies see footnote e of Table 3.

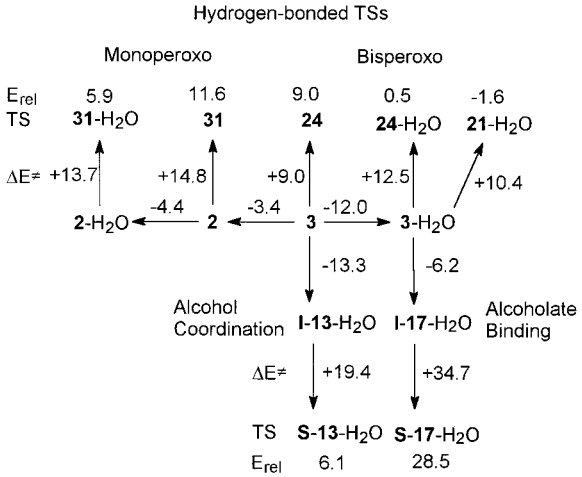

Figure 8. Relative energies (E_{rel}, kcal/mol) of epoxidation transition structures relative to **3** + H_2O + propenol. Figures with plus signs near arrows report the corresponding activation energies ($\Delta E^{\ddagger}$, kcal/mol). Other figures with minus signs near arrows indicate the formation energies (kcal/mol) of **2**, the hydrated complexes **2**-H_2O and **3**-H_2O, as well as the intermediates **I-13**-H_2O and **I-17**-H_2O.

followed by an easy and stereocontrolled intramolecular oxygen delivery by the peroxo group to the olefinic double bond, and (iii) an intermolecular oxygen-transfer process assisted by a hydrogen-bonding interaction with the rhenium complex as hydrogen bond acceptor and HOR as hydrogen bond donor.

The most stable TSs for each mechanism are reported in Figure 8 to facilitate a fast comparison among relative energies (E_{rel}) and activation barriers ($\Delta E^{\ddagger}$).

Calculations clearly suggest that the reaction routes starting both from coordination of propenol and from formation of a metal alcoholate are viable reaction channels. However, along these routes the reacting systems have to surmount very high first order saddle points so that these pathways do not contribute appreciably to epoxide formation.

As for the third mechanism, via hydrogen-bonded transition structures, our calculations demonstrated that Re−bis(peroxo) complexes (both unsolvated and hydrated derivatives) are more reactive than the corresponding Re−monoperoxo complexes, in substantial accord with kinetic studies by Espenson et al.[24]

A careful computational study of the "front-side" electrophilic attack by the unsolvated Re−bis(peroxo) complex on propenol led to the following conclusions:

□ several (eight) TSs can compete with each other in the formation of the final epoxide,

□ transfer of electronic charge (about −0.35 e) takes place from propenol mostly to both oxygens of the attacking peroxo system,

□ in syn TSs the stabilizing hydrogen-bonding interaction (some kcal/mol) overcompensates the rate-retarding electron-withdrawing effect of the OH group,

□ hydrogen bonding can involve, as hydrogen bond acceptors, not only the oxygen atoms of the reacting or nonreacting peroxo moieties (the former TSs are slightly more stable than the latter ones), but also the oxo oxygen (these TSs are the least stable ones),

□ the approach geometry of the Re complex to the double bond is rather flexibile, and in some instances a sizable rotation (from the inherently optimal disposition observed in the ethene reaction) around the attacking O_4-O_5 direction occurs to maximize hydrogen bonding,

□ all TSs can be characterized as "spiro-like" structures in which the plane of the attacking peroxo moiety is closer to a perpendicular (90°) than to a coincident (0°, "planar") orientation with respect to the plane of the oxirane being formed, and

□ the allylic OH can adopt either an "inside" or an "outside" conformation.

All of these observations substantially hold also for TSs derived from the reaction of the hydrated Re−bis(peroxo) complex with propenol. Interestingly, in the case of solvated TSs, those with hydrogen bonding to the attacking peroxo group are definitely more stable than other TSs with hydrogen bonding either to the nonreacting peroxo moiety or to the oxo functionality. Water coordination strongly lowers the energy of the TSs compared to that of their unsolvated counterparts. However, this large energy gap can, at least to a significant extent, be compensated for by counterbalancing entropic effects.

In conclusion, computational data suggest that the Re−bis(peroxo) complex (most probably the hydrated form) is the active species, in the catalyzed hydrogen peroxide epoxidation of propenol, via spiro-like TSs with hydrogen bonding to the attacking peroxo fragment and with the OH group either in an "outside" or "inside" conformation. Our study corrects previous qualitative TS models and provides experimentalists with a sound and reliable basis for mechanistic discussions of Re-catalyzed epoxidation of allylic alcohols.

Acknowledgment. We thank MURST and CNR (Italy) as well as the Deutsche Forschungsgemeinschaft and the Fond der Chemischen Industrie (Germany) for financial support.

Supporting Information Available: Geometries (either Z-matrixes or cartesian coordinates) for all of the structures reported. Structural data of the TSs for propene and propenol epoxidation with **3**. Electronic energies of reactants, intermediates and TSs. Vibrational ZPE for TSs. This material is available free of charge via the Internet at http://pubs.acs.org.

JA003868Y